CBPF-NF-082/96

Electronic Structure and Hyperfine Properties of Molecules and Solids by Cluster Methods

Diana Guenzburger

Centro Brasileiro de Pesquisas Físicas - CBPF
Rua Dr. Xavier Sigaud, 150
22290-180 – Rio de Janeiro, RJ – Brasil

Abstract

The numerical first-principles Discrete Variational method in the framework of Density Functional theory is a flexible tool to be used in the investigation of the electronic structure of large molecules, and of clusters of atoms representing solid-state systems, with or without translational symmetry. Results are presented for the nanoscale antiferromagnet $[Fe(OCH_3)(OCCH_2Cl)]_{10}$ (the "ferric wheel" molecule), the layered compounds $RENi_2B_2C$ (RE $\equiv$ rare earth), and for the metallic systems $\gamma-$Fe and particles of $\gamma-$Fe in a Cu matrix. Hyperfine properties are also derived from the self-consistent electron densities obtained.

1 Introduction

First-principles methods based on Density Functional theory (DFT) [1] provide accurate and relatively fast means to abtain the electronic structure and properties of solids and molecules. The Local Density approximation (LDA) has been employed to investigate solids in two types of approaches. If the solid has translation symmetry, as in a pure crystal, Bloch theorem applies, which states that the one-electron function ϕ_i at point $(\vec{r} + \vec{R})$, where $\vec{R}$ is a lattice vector, is equal to the function at point $\vec{r}$ times a phase factor:

$$\phi_i(\vec{r} + \vec{R}) = e^{i\vec{k}\cdot\vec{R}}\phi_i(\vec{r}) \tag{1}$$

Based on this property the band-structure methods were generated [2], in which the electronic structure is obtained in $\vec{k}$ space. LDA band-structure methods may often be recognized by their initials, such as APW, LMTO, FLAPW, KKR, etc.

However, if translational symmetry is missing, band-structure calculations are not possible. This is the case of free molecules, and of solids with impurities (substitutional or interstitial), vacancies, local geometry distortions, etc. For these cases, DFT methods are applied in real space. The Discrete Variational Method (DVM) [3] is an all-numerical self-consistent scheme in which the one-electron wave functions are expanded on a basis of numerical atomic orbitals (NAO). These features make the DVM less computer-time consuming than the Gaussian-basis counterparts, and thus suitable for large molecules and for clusters of atoms representing solid-state systems. Heavy atoms may be included, such as transition metals and lanthanides. In the case of clusters, an embedding scheme is considered, to simulate the environment in the solid.

In what follows, a summary of the main features of the method will be given (Section 2), and examples of current applications (Section 3), which include the "ferric wheel" molecule $[Fe(OCH_3)(OCCH_2Cl)]_{10}$, the layered compounds $RENi_2B_2C$, some of which are superconductors, and the metallic systems $\gamma-$Fe (or fcc Fe) and $\gamma-$Fe particles in a Cu matrix.

2 Summary of the Theoretical Method

In the DVM method [3] in Kohn-Sham equations of DFT are solved for the cluster or the molecule in a three-dimensional grid of points (in hartrees):

$$(-\nabla^2/2 + V_c + V_{xc}^{\sigma})\phi_{i\sigma} = \varepsilon_{i\sigma}\phi_{i\sigma} \tag{2}$$

where V_c is the Coulomb potential of nuclei and electrons and V_{xc}^{σ} is the exchange-correlation potential for spin σ [4], a functional of the electron density of spin σ:

$$\rho_{\sigma}(\vec{r}) = \sum_i n_{i\sigma}|\phi_{i\sigma}(\vec{r})|^2 \tag{3}$$

In spin-polarized calculations $\rho_{\uparrow}(\vec{r})$ may be different from $\rho_{\downarrow}(\vec{r})$, thus allowing the exchange interaction to create a spin-polarization. The molecular or cluster spin-orbitals ϕ_i are expanded on a basis of NAO orbitals, which are obtained by numerical atomic self-consistent LDA calculations. The NAO basis may be improved by considering atoms with the configuration as in the molecule or cluster; this is obtained by a Mulliken-type population analysis.

The Discrete Variational scheme leads to the secular equations which are solved self-consistently in the three-dimensional numerical grid:

$$([\mathrm{H}]-[\mathrm{E}][\mathrm{S}])[\mathrm{C}] = 0 \tag{4}$$

In Eq. 4, [H] is the Hamiltonian matrix, [S] the overlap matrix and [C] the matrix of the coefficients which define ϕ_i. The numerical grid is pseudo-random (Diophantine) except inside spheres around certain atomic nuclei, where a precise polynomial integration is performed. The total number of points per atom varies from 200-300 for small atoms such as C or O, to several thousands for larger atoms such as transition metals and lanthanides.

In the case of clusters representing solids, the embedding is constructed by placing eletron densities obtained by LDA atomic calculations at the sites of several shells of atoms in the surrounding crystal. In the atomic calculations, configurations of the atoms as obtained self-consistently for the cluster are considered. The external electron densities are added to the cluster density to build the cluster Hamiltonian.

To facilitate the evaluation of the Coulomb term, a model density consisting of a multicenter multipolar expansion is used in the Hamiltonian; this is fitted to the "real" density by a least-squares procedure [5].

Non-local corrections to the exchange and correlation potential may be employed [6], in calculations involving the total electronic energy.

3 Electronic Structure and Properties

3.1 The "ferric wheel" molecule

In recent years, there has been considerable effort in constructing and investigating the properties of systems of nanoscale or mesoscopic dimensions, containing a finite number of magnetic transition-metal atoms [7]. Such systems are in the bordeline of isolated and collective magnetic behavior, and some present new and interesting magnetic effects: superparamagnetism, tunnelling between magnetic states, etc. [8].

Large systems of magnetic transition metals may be obtained by chemical synthesis of polynuclear organo-metallic molecules [9], [10]. The organic ligands encapsulate the core containing the transition metals, such that magnetic interactions are confined within the molecule.

The molecule $[Fe(OMe)_2(O_2CCH_2Cl)]_{10}$ denominated "ferric wheel" is one of these systems, in which the ten Fe atoms in circular disposition have their spins coupled anti-ferromagnetically forming a S=0 ground state [9]. Mössbauer hyperfine parameters were reported. The electronic structure was obtained with the DVM method [11]. The atomic basis included 3s, 3p, 3d, 4s and 4p for Fe, 2s and 2p for C and O. The terminal H and Cl atoms were not considered, to maintain D_5 point symmetry. Inner orbitals were kept frozen throughout the SCF calculations, after being explicitly orthogonalized against the valence. The number of points used were 5,500 for each Fe atom and 420 for C and O. In Figs. 1a and 1b are displayed schematic views of the cluster $[Fe(OC)_2(O_2CC)]_{10}$ representing the "ferric wheel" molecule.

In Table 1 are given the self-consistent magnetic moments and populations of the Fe atoms in the "ferric wheel". The total charge on Fe is +2.2, and the total spin moment $4.3\mu_B$. This shows that Fe in an intermediate oxidation state between +2 and +3.

The quadrupole splitting QS of the excited state of the 14.4 keV transition of ^{57}Fe is given by

$$QS = 1/2eV_{zz}Q\left(1+\frac{\eta^2}{3}\right)^{1/2} \qquad (5)$$

where Q is the quadrupole moment of the nucleus in the excited state (I=3/2) of the Mössbauer transition, V_{zz} the electric field gradient and η the asymetry parameter. The components of the electric field gradient tensor are calculated from the SCF molecular density $\rho(\vec{r})$ by [12]:

$$\begin{aligned} V_{ij} &= -\int \rho(\vec{r})(3x_i x_j - \delta_{ij} r^2)/r^5 dv + \\ &+ \sum_q Z_q^e (3x_{qi} x_{qj} - \delta_{ij} r_q^2)/r_q^5 \end{aligned} \tag{6}$$

The first term is the electronic contribution and the second term the contribution of the surrounding nuclei shielded by the core electrons, with effective charge Z_q^e. After diagonalization, the electric field gradient V_{zz} is defined by the convention:

$$[V_{zz}| > |V_{yy}| \geq |V_{xx}]$$

with

$$\eta = \frac{V_{xx} - V_{yy}}{V_{zz}} \tag{7}$$

Employing the value Q =0.16b [13], we obtained $QS = +0.73$ mm/s, to be compared to 0.62 mm/s obtained experimentally [9]. The sign was not measured in the experiment.

3.2 The quaternary layered compounds $RENi_2B_2C$

The compounds $RENi_2B_2C$ (RE≡ rare earth) have been synthetized recently and raised great interest due to the fact that some of them exhibit superconducting properties [14]. Moreover, among them may be found examples of coexistence of superconductivity and magnetism. The compounds have structures formed by layers of RE−C intercalated with layers of B and of Ni.

Self-consistent calculations for embedded clusters of around 70 atoms representing the compounds were performed with the DVM method [15] – [18], for several rare-earth (Y, Pr, Nd, Sm, Gd, Tb, Dy, Ho, Er). The 4f orbital of the lanthanide was kept in the variational space. In Fig. 2 is shown a representation of a typical cluster. Moreover, substitution of one or several Ni atoms by Fe, Co and Ru was also considered [15], [18].

One puzzling aspect was the fact that only compounds containing heavier rare-earths (Dy, Ho, Er and Tm) exhibit superconductivity, whereas those with lighter RE do not. An explanation for this was derived through the calculations. It was found that the

spin-polarization of the conduction electrons by the RE 4f spin moment is much more effective in the case of the lighter RE than in the heavier, due to the larger radius of the 4f orbital in the early lanthanides [16], [17]. It is known that spin-polarization destroys superconductivity through the exchange field, by destabilizing the Cooper pairs.

Quadrupole Splittings were obtained in the case of Fe-substituted $RENi_2B_2C$ (RE=Y, Gd, Tb, Dy, Ho, Er) [18], and compared to experimental values measured by Mössbauer spectroscopy. The results are displayed in Fig. 3. Considering the complexity of the systems, the agreement may be considered very good.

3.3 $\gamma-$Fe and $\gamma-$Fe particles in Cu

Pure bulk fcc(γ) Fe only exists at very high temperatures (between 1183 and 1667 K). However, fcc Fe may be stabilized down to very low temperatures either as small $\gamma-$Fe coherent preciptates in a Cu or Cu-alloy matrix, or as thin epitaxial films on a Cu substrate [19]. There is great interest in $\gamma-$Fe due to the existance of several low-lying magnetic states, which has been related to the INVAR effect found in many $\gamma-$Fe-based alloys.

The DVM method was employed to investigate the electronic structure of $\gamma-$Fe in antiferromagnetic (AFM) and ferromagnetic (FM) spin configirations [20]. The effect of variations in the lattice parameter on the Fe spin moments and on the magnetic Hyperfine Fields was assessed, by performing calculations at several interatomic distances. The solids were represented by cubic embedded clusters containing 62 atoms.

In order to investigate the effect of the copper matrix in the $\gamma-$Fe particles, calculations were performed for embedded cubic clusters containing 14 Fe atoms (representing the particle) surrounded by 48 Cu atoms, in the fcc geometry [21]. In Fig. 4 is shown a representation of the cluster $Fe_{14}Cu_{48}$. The polarization of the surrounding Cu atoms by the Fe atoms may be visualized through spin-density $[\rho_\uparrow(\vec{r}) - \rho_\downarrow(\vec{r})]$ contour maps. In Fig. 5 is seen the spin density of the FM Fe particle surrounded by Copper. The results show that the Cu atoms 3d orbitals polarized parallel to the Fe 3d, and the Cu 4p polarize antiparallel. This may also be seen by a Mulliken population analysis for spin up and spin down electrons.

4 Conclusions

The Discrete Variational Method based on Density Functional theory is a flexible tool which allows to obatin the electronic structure of large transition metal molecules, as well as large embedded-clusters representing solid state systems. The molecule $[Fe(OMe)_2(O_2CCH_2Cl)]_{10}$ ("ferric wheel") was investigated, the magnetic moment and charge on the Fe were obtained, as well as the Quadrupole Splitting, calculated to be +0.73 mm/s. Embedded clusters of ~ 70 atoms were considered to represent the layered compounds $RENi_2B_2C$, pure and substituted with Fe, Co and Ru. In the case of a single Fe substitution, representing a dilute impurity substituting for Ni, Quadrupole Splittings were calculated and compared to Mössbauer Spectroscopy Measurements. Finally, pure $\gamma-$Fe in the FM and AFM magnetic configurations, and $\gamma-$Fe particles in a Cu matrix, were represented by 62-atoms embedded clusters. Magnetic properties were derived by Mulliken-type populations analysis and by spin-density maps.

Acknowledgements

Calculations were performed at the Cray YMP of the Supercomputing Center of the Universidade Federal do Rio Grande do Sul, and at the Cray J90 of COPPE/Federal University of Rio de Janeiro.

Table 1

Mulliken-type populations, net charges and magnetic moments μ of Fe in cluster $[Fe(OC)_2(O_2CC)]_{10}$. Magnetic moments are for Fe atoms with positive spin.

	Population			Magnetic Moment (μ_B)
	$\uparrow$ ($m_s = 1/2$)	$\downarrow$ ($m_s = -1/2$)	total	
3d	4.84	0.60	5.44	4.24
4s	0.07	0.03	0.09	0.04
4p	0.09	0.07	0.15	0.02
			net charge:+2.32	total:4.30

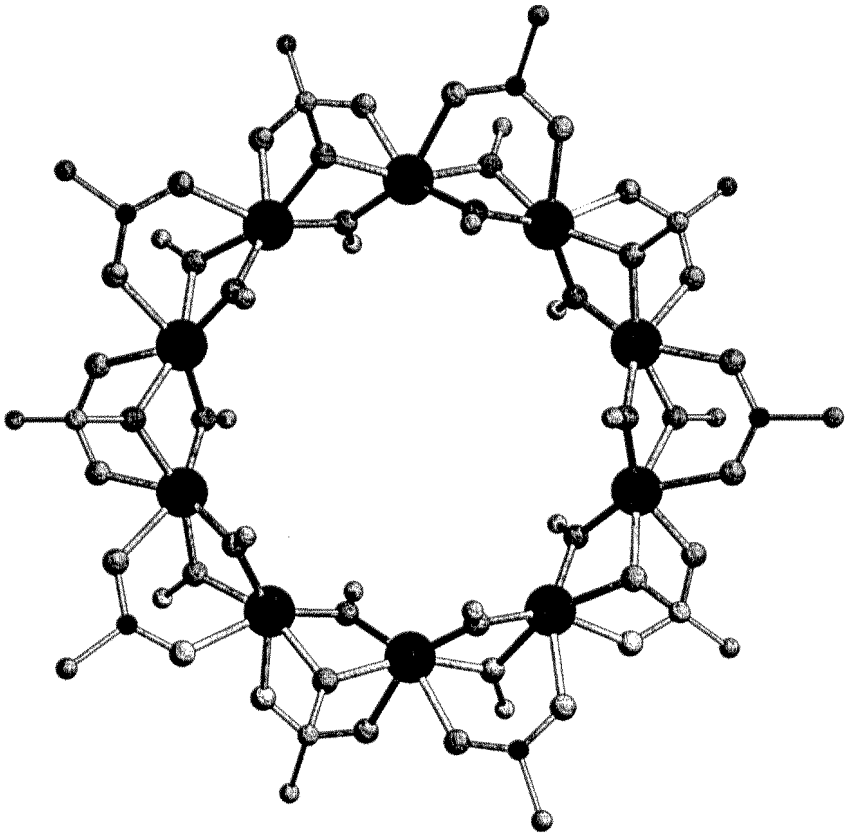

Figure 1a – Top view of the molecule $[Fe(OMe)_2(O_2CCH_2Cl)]_{10}$. The terminal H and Cl atoms have been excluded.

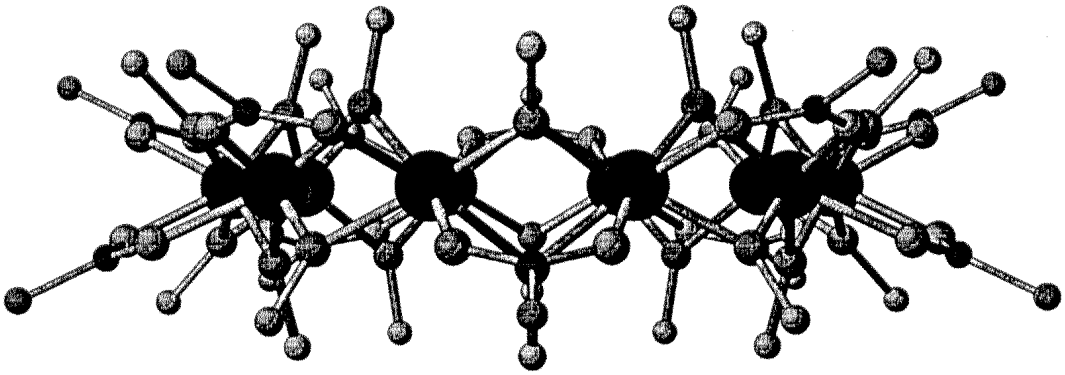

Figure 1b – Side view of $[Fe(OMe)_2(O_2CCH_2Cl)]_{10}$ with H and Cl atoms excluded.

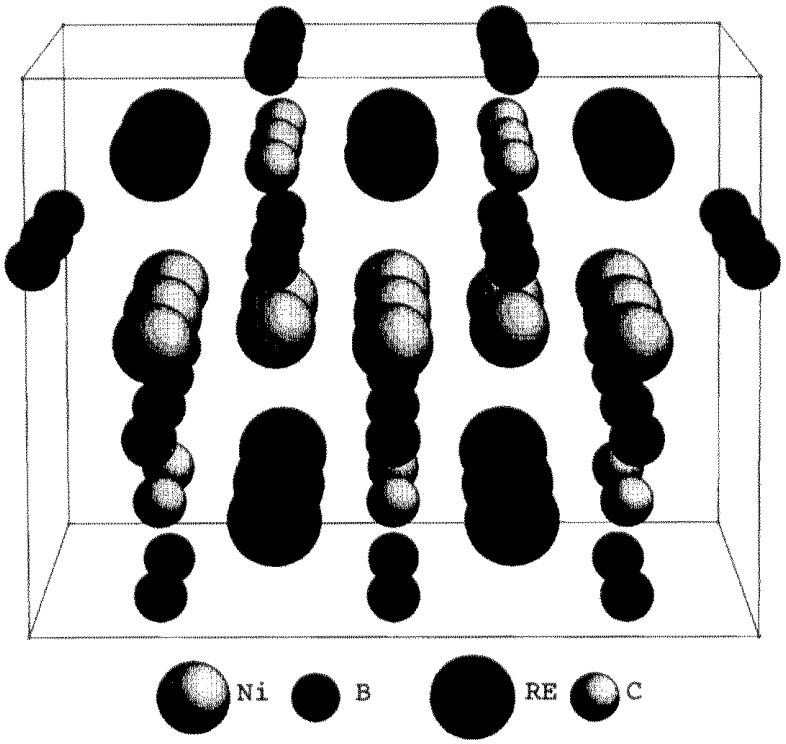

Figure 2 – Cluster representing the compounds $RENi_2B_2C$.

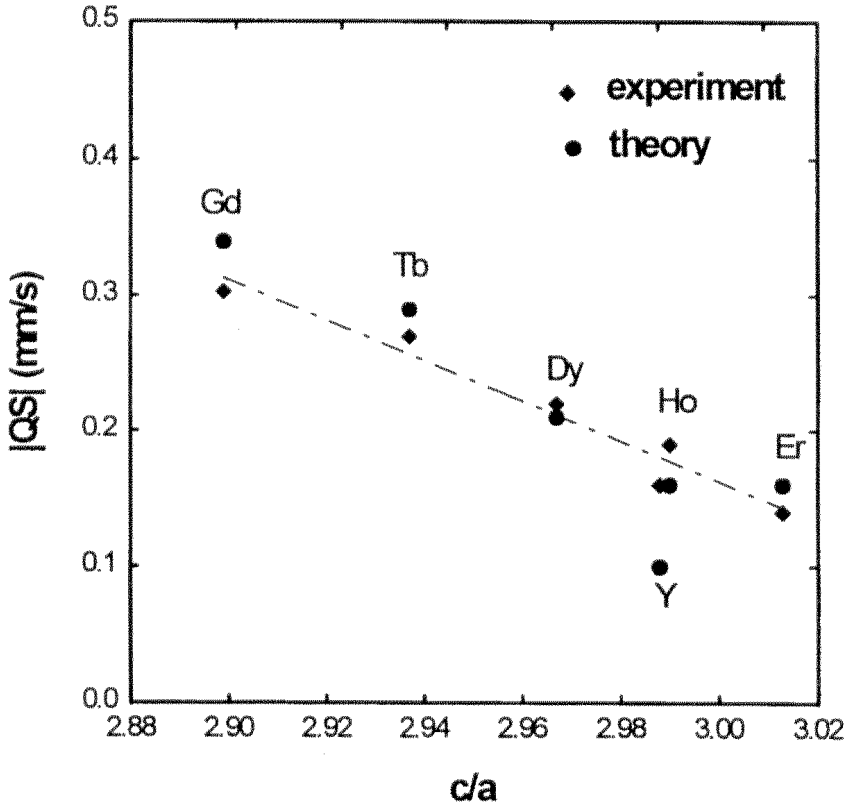

Figure 3 – Experimental and calculated absolute values of the quadrupole splitting (|QS|) at the Fe nucelus in the compounds $RE(Ni_{0.99}Fe_{0.01})_2B_2C$, correlated to the ratio of the lattice parameters c/a. Q (^{57}Fe)=0.16b (from Ref. [13]). Dotted line is to guide the eye. Clusters representing the solids are: $RE_{12}Fe_1Ni_{14}B_{32}C_{12}$. The Fe impurity is placed at the center, substituting one Ni atom. From ref. [11].

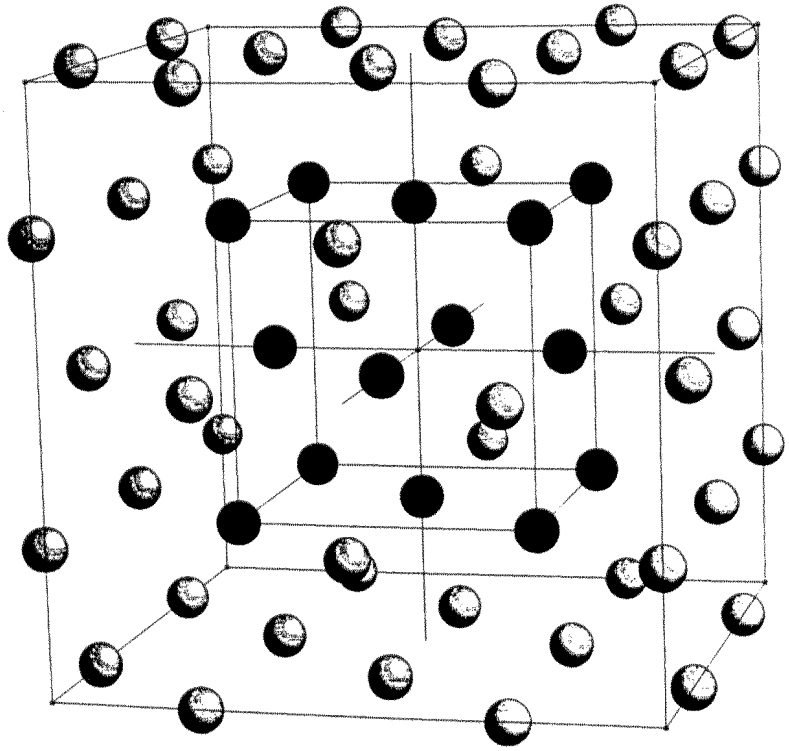

Figure 4 – $Fe_{14}Cu_{48}$ cluster representing a Fe particle in copper. Darker shade spheres represent Fe.

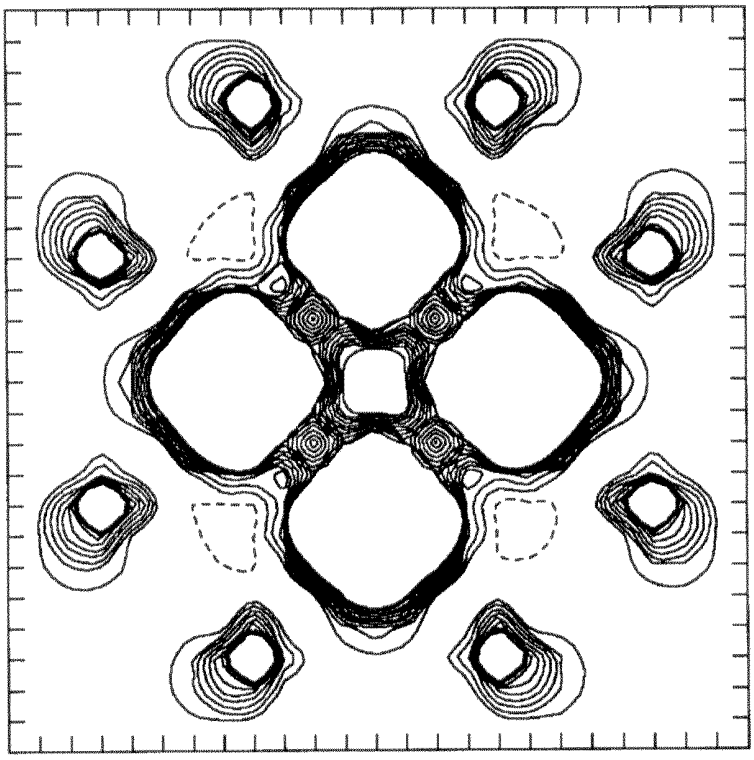

Figure 5 – Spin density contours for a FM γ–Fe particle surrounded by copper in the (011) plane represented by the cluster $Fe_{14}Cu_{48}$. Contours are from -0.01 to $+$ 0.01 e/a.u.^{3} with intervals of 0.001 e/a.u.^{3} Full lines are positive values. From ref. [21]

References

[1] see, for example: R.G. Parr and W. Yang, "Density Functional Theory of Atoms and Molecules", Oxford University Press, N. York (1989).

[2] See for example, J. Callaway, "Energy Band Theory", "Pure and Applied Physics" monograph no. 16, Academic Press, N. York (1964).

[3] D.E. Ellis and J. Guo in "Electronic Density Functional Theory of Molecules, Clusters and Solids", ed. by D.E. Ellis, (Kluwer, Dordrecht, 1994); D.E. Ellis and G.S. Painter, Phys. B **2**, 2887 (1970).

[4] U. von Barth and L. Hedin, J. Phys. C **5**, 1629 (1972).

[5] B. Delley and D.E. Ellis, J. Chem. Phys. **76**, 1949 (1982).

[6] A.D. Becke, Phys. Rev. A **38**, 3098 (1988); J.P. Perdew, Phys. Rev. B **33**, 8822 (1986); ibid B **34**, 7406 (1986).

[7] D.D. Awschalom and D.P. DiVincenzo, Physics Today **48**, 43 (1995).

[8] D.D. Awschalom, D.P. Di Vincenzo and J.F. Smyth, Science **258**, 414 (1992).

[9] K.L. Taft and S.J. Lippard, J. Am. Chem. Soc. **112**, 9629 (1990) K.L. Taft, C.D. Delfs, G.C. Papaefthymiou, S. Foner, D. Gatteschi and S.J. Lippard, J. Am. Chem. Soc. **116**, 823 (1994).

[10] G.C. Papaefthymiou, Phys. Rev. B**46**, 10366 (1992).

[11] Z. Zeng, Y. Duan and D. Guenzburger, unpublished.

[12] J. Terra and D. Guenzburger, Phys. Rev. B **44**, 8584 (1991).

[13] P. Dufek, P. Blaha and K. Schwarz, Phys. Rev. Letters **75**, 3545 (1995).

[14] R.J. Cava et al., Nature **367**, 146 (1994); R.J. Cava et al, ibid **367**, 252 (1994).

[15] Z. Zeng, D.E. Ellis, D. Guenzburger and E.B. Saitovitch, Phys. Rev. B **53**, 6613 (1996).

[16] Z. Zeng, D.E. Ellis, D. Guenzburger and E.B. Saitovitch, Phys. Rev. B, in press.

[17] Z. Zeng, D. Guenzburger, D.E. Ellis and E.B. Saitovitch, Physica C, in press.

[18] Z. Zeng, D.R. Sánchez, D. Guenzburger, D.E. Ellis, E.B. Saitovitch and H. Micklitz, Phys. Rev. B, in press.

[19] W. Keune, T. Ezawa, W.A.A. Macedo, U. Glos and K.P. Schletz, Physica B **161**, 269 (1989).

[20] D. Guenzburger and D.E. Ellis, Phys. Rev. B **51**, 12519 (1995).

[21] D. Guenzburger and D.E. Ellis, Phys. Rev. B **52** 13390 (1995).